06

Influence of Cr content in TiCrN coatings obtained by vacuum arc deposition on their phase composition, structure and properties

© A.A. Leonov[1], Yu.A. Denisova[1], V.V. Denisov[1], M.S. Syrtanov[1,2]

[1] Institute of High Current Electronics, Siberian Branch, Russian Academy of Sciences, Tomsk, Russia
[2] Tomsk Polytechnic University, Tomsk, Russia
E-mail: laa-91@yandex.ru

Received March 24, 2025
Revised June 17, 2025
Accepted July 8, 2025

The TiCrN coatings were deposited on Cr12MoV die steel using the vacuum-arc plasma-assisted method at different values of the chromium cathode arc current (40, 60, 80 and 100 A). It was found that an increase in the chromium cathode arc current leads to an increase in the relative chromium content in the coatings from 0.26 to 0.52; an increase in the content of the (Ti, Cr)N phase from 18.3 to 94.2 %; a decrease in the coherent scattering regions size from $\sim 30-40$ to ~ 5 nm; an increase in the microstrains of crystal lattices from $(0.8-1.6)\cdot 10^{-3}$ to $(10-11.1)\cdot 10^{-3}$. The $Ti_{0.54}Cr_{0.46}N$ coating had the highest mechanical (hardness $H = 37.4$ GPa, ratio of hardness and elastic modulus $H^3/E^2 = 0.30$ GPa) and tribological (friction coefficient $\mu = 0.512$) characteristics among the studied coatings.

Keywords: vacuum arc deposition, TiCrN coatings, phase composition, mechanical properties.

DOI: 10.61011/TPL.2025.10.62111.20322

Transition metal nitrides, such as TiN and CrN, are used widely as protective hardening coatings in various industries due to their relatively high hardness and reasonably low friction coefficient, which provide an opportunity to extend the service life of products in abrasive and chemically aggressive conditions [1–3]. However, these simple mononitride coatings fail quickly if the coated product is exposed to more severe influences that cause intensive wear [4,5]. Three-component systems (e. g., TiCrN) have improved physical, mechanical, and tribological properties compared to mononitride TiN and CrN, which expands their application range. For example, it was demonstrated in [6] that a TiCrN film had significantly better tribological characteristics than TiN. Comparing the results of wear tests under a load of 3 N, the authors found that the friction coefficient of the TiCrN film decreased by a factor of more than 3.5, while the wear parameter decreased by a factor of more than 11 (compared to TiN).

A certain structure and phase composition form depending on the method and mode of synthesis of TiCrN coatings/films and on the relative content of chromium. They, in turn, govern the physical, mechanical, and tribological properties of coatings/films and, accordingly, specify the service life of the product to which this coating/film is applied. TiCrN films in [7] were deposited by the cathodic arc PVD method. It was found that as the chromium content in TiCrN films increased, the phase composition changed from cubic TiN to cubic CrN with the formation of substitution solid solutions TiN(Cr) and CrN(Ti). It was also reported that a TiCrN film with $Cr/Ti = 0.587$ exhibited higher wear resistance and compressive residual stresses than films with $Cr/Ti = 0.428$, 0.754, 0.923, 1.083, and 2.571. In [8], coatings of the Ti−Cr−N composition were synthesized by vacuum arc deposition. The authors found that both an increase in microhardness (as large as 70 % compared to mononitride titanium nitride coatings) and a reduction of friction coefficient (as large as 50 %) could be achieved by increasing the chromium concentration to 17 at.%. This improvement of physical and mechanical properties of Ti−Cr−N coatings was attributed to the formation of a (Ti,Cr)N solid solution with the $B1$ NaCl structure and a coherent scattering region (CSR) size of 10 nm. The above suggests that the Cr content of TiCrN coatings needs to be optimized in order to maximize the physical, mechanical, and tribological parameters. In this context, the present study was aimed at examining the influence of the relative content of Cr in TiCrN coatings deposited using the vacuum-arc plasma-assisted method on their phase composition and crystal structure parameters and identifying the optimum coating composition with the best physical, mechanical, and tribological characteristics.

A modernized NNV6.6-I1 [9] setup fitted with two electric arc evaporators with a cathode diameter of 80 mm and an additional source of gas plasma (plasma source with a heated and hollow „PINK“ cathode) was used to deposit coatings by the vacuum-arc plasma-assisted method. Cathodes made of titanium (grade VT1-0) and chromium (99.5 % pure) were used. Pre-hardened die steel Cr12MoV was the substrate material. The samples were polished in advance and cleaned in an ultrasonic bath (first in gasoline, then in acetone) prior to loading into the vacuum chamber. In the process of deposition, the sample holder was rotated about the central axis of the chamber at a distance of 200 mm from it at a rate of 3.5 rpm and about its own axis. When a gas discharge was ignited and a negative bias potential of 700 V was applied to the holder with

the substrates, heating to a temperature of approximately 360 °C was performed. Upon reaching this temperature, the surface of substrates was treated with Cr ions for 2 min under a negative substrate potential of 900 V, a chromium cathode arc current of 90 A, and pressure $P_{Ar} = 0.35$ Pa. An adhesion layer of Cr was then deposited within 3 min under a negative substrate potential of 50 V. TiCrN coatings were deposited next in a nitrogen–argon gas mixture (90 % N_2 and 10 % Ar) under a pressure of 0.6 Pa and a negative potential of 150 V with simultaneous arcing of Ti and Cr cathodes. The titanium cathode arc current was 80 A for all deposited TiCrN coatings, and the chromium cathode arc current was varied (40, 60, 80, or 100 A). A higher chromium cathode arc current corresponded to a higher coating growth rate. To maintain a constant thickness of the studied TiCrN coatings, the coating deposition time was set to 95, 85, 75, and 65 min at 40, 60, 80, and 100 A, respectively. In all experiments, the temperature was maintained at 390−400 °C. The temperature in the vacuum chamber was monitored with a chromel-alumel thermocouple mounted in a special holder, which was positioned in the center of the chamber. For a comparative analysis of the properties of coatings, base mononitride TiN and CrN coatings were deposited under similar conditions, but the deposition time of each coating was set to 120 min. The approximate thickness of all the coatings studied was 3−4 μm. The elemental composition of coatings was examined with a Genesis energy-dispersive X-ray microanalyzer built into a Philips SEM-515 (Netherlands) scanning electron microscope. The phase composition and parameters of the crystal structure of the obtained coatings were studied by X-ray diffraction using a Shimadzu XRD-7000S (Japan) diffractometer with CuK_α ($\lambda = 0.15405$ nm) radiation. Diffraction patterns were recorded with the following process parameters: step, 0.0143°; exposure, 21 s; angle range, from 10 to 90°. The Crystallographica Search-Match program and the ICDD (International Centre for Diffraction Data) databases were used in qualitative analysis of these patterns. Quantitative analysis (determination of the CSR size, microstrains of the crystal lattice, and lattice parameters) was carried out using the Powder Cell 2.4 full-profile analysis program. Nanoindentation of the studied coatings was performed using an NHT-S-AX-000X (Germany) nanohardness tester with a Berkovich tip under a maximum load of 25 mN. Ten measurements were taken for each coating. Tribological tests were carried out using a TRIBOtechnic (France) tribometer under dry friction conditions with reciprocal motion of the sample relative to the counterbody. The counterbody was a ball 6 mm in diameter made from hardened steel 100Cr6. The sample displacement rate during testing was 25 mm/s, the load on the ball was 5 N, and the track length was 5 mm; the sliding distance was 200 m for TiCrN and CrN coatings and 50 m for the TiN coating. The sliding distance for TiN had to be shortened due to the fact that this coating wore out rapidly.

Table 1 presents the elemental composition of the studied TiCrN coatings. The results demonstrate that with an increase in chromium cathode arc current from 40 to 100 A, the chromium content of the coatings increases from 13.6 to 29.3 at.

Figure 1 shows the X-ray diffraction patterns of the studied TiCrN and mononitride TiN and CrN coatings. It was found that the base mononitride TiN and CrN coatings consist of titanium nitride (ICDD card 87-631) and chromium nitride (ICDD card 76-2494) with an FCC structure of the NaCl type and a preferential (111) orientation. The intensity of diffraction peak (222) was very low for both TiN and CrN coatings. Other reflection planes, such as (220) and (311), were almost indistinguishable in the diffraction patterns. TiCrN coatings had a three-phase structure with FCC lattices that included the TiN and CrN phases, which were the primary phases in mononitride coatings, and a newly formed (Ti,Cr)N substitutional solid solution phase (ICDD card 70-2981). The same (111) texture observed in mononitride coatings was found in TiCrN coatings. The diffraction patterns of TiCrN coatings make it evident that an increase in relative content of chromium in them leads to a shift of peaks toward larger diffraction angles 2θ (i. e., the lattice parameter of coatings decreases). Indeed, it follows from the data in Table 2 that the values of lattice parameter a of the (Ti,Cr)N, TiN, and CrN phases tend to decrease. The reduction of the lattice parameter of (Ti,Cr)N with an increase in relative content of chromium in the coatings is attributable to the substitution of Ti with Cr in the TiN lattice, since the atomic radius of Cr (0.130 nm) is smaller than that of Ti (0.147 nm). A similar shift of peaks toward larger angles in TiCrN coatings with an increase in relative chromium content was observed in [10], and the authors associated it with rapid formation of the (Ti,Cr)N solid solution. It can be seen from Table 2 that an increase in relative chromium content in TiCrN coatings leads to an increase in (Ti,Cr)N phase content, which changes from 18.3 to 94.2 %. The diffraction patterns of TiCrN coatings (Fig. 1) also demonstrate that an increase in relative chromium content leads to broadening of the diffraction peaks and a reduction in their intensity, which is indicative of a reduction in CSR size. The CSR size decreases from $\sim 30-40$ to ~ 5 nm (see Table 2). An increase in chromium cathode arc current does not only lead to an increase in Cr content in TiCrN coatings, but also promotes more intense ion bombardment of the deposited coating surface, which initiates refinement of the coating structure and contributes to an increase in defect density and an enhancement of compressive stresses in the coating [11].

Table 1. Elemental composition of the studied TiCrN coatings

Sample	Element concentration, at.%		
	Ti	Cr	N
$Ti_{0.74}Cr_{0.26}N$	38.5	13.6	47.9
$Ti_{0.63}Cr_{0.37}N$	31.9	18.8	49.3
$Ti_{0.54}Cr_{0.46}N$	27.8	23.3	48.9
$Ti_{0.48}Cr_{0.52}N$	27.4	29.3	43.2

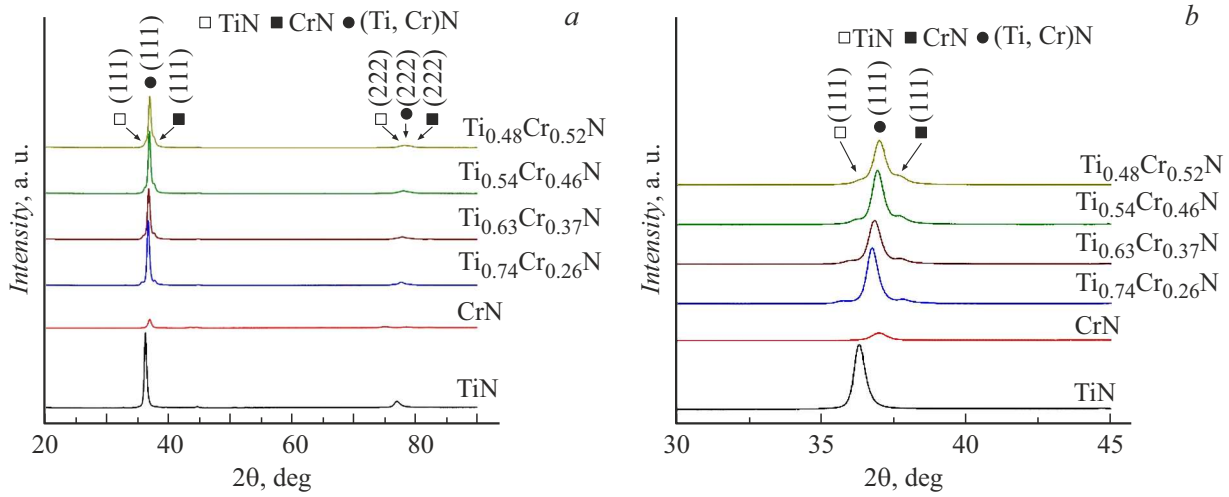

Figure 1. X-ray diffraction patterns of the studied TiCrN coatings and mononitride TiN and CrN coatings within the angular range of 20−90 (*a*) and 30−45° (*b*).

Table 2. Phase composition and parameters of the crystal structure of the studied TiCrN coatings ($\Delta d/d$ — microstrain of the crystal lattice)

Parameter	Phase	Sample			
		$Ti_{0.74}Cr_{0.26}N$	$Ti_{0.63}Cr_{0.37}N$	$Ti_{0.54}Cr_{0.46}N$	$Ti_{0.48}Cr_{0.52}N$
Phase content, %	(Ti,Cr)N	18.3	67.3	74.6	94.2
	TiN	78.3	13.6	–	< 1
	CrN	3.5	19.2	25.4	5.5
CSR size, nm	(Ti,Cr)N	31.4	17.9	9.5	–
	TiN	39.5	5.1	–	–
	CrN	36.1	39.0	3.5	5.4
$\Delta d/d$, 10^{-3}	(Ti,Cr)N	1.6	2.9	3.3	–
	TiN	1.3	5.9	–	–
	CrN	0.8	0.4	10.1	11.1
Parameter parameter a, nm	(Ti,Cr)N	0.418	0.414	0.413	0.413
	TiN	0.424	0.425	–	–
	CrN	0.414	0.412	0.404	0.405

Specifically, it follows from Table 2 that an increase in arc current led to an increase in microstrains of the crystal lattice ($\Delta d/d$) of phases: (Ti, Cr)N — from $1.6 \cdot 10^{-3}$ to $3.3 \cdot 10^{-3}$; TiN — from $1.3 \cdot 10^{-3}$ to $5.9 \cdot 10^{-3}$; CrN — from $0.8 \cdot 10^{-3}$ to $11.1 \cdot 10^{-3}$.

The physical and mechanical properties of the coatings were examined by nanoindentation. The hardness (H) and elastic modulus (E) values were determined (Table 3) using specialized software. The ratios of hardness and elastic modulus (H/E and H^3/E^2) of the studied coatings were also calculated and are listed in Table 3. It can be seen from Table 3 that the CrN mononitride coating has the minimum hardness (23.8 GPa) among the studied coatings. The $Ti_{0.54}Cr_{0.46}N$ coating had the maximum hardness (37.4 GPa), which was 21 and 57 % higher than that of the TiN and CrN mononitride coatings, respectively. The increased hardness of the $Ti_{0.54}Cr_{0.46}N$ coating is attributable to a smaller CSR size and higher microstrain values [12].

It is believed that ratio H/E is a measure of elastic-strain-to-break and ratio H^3/E^2 characterizes the capacity of the surface to resist plastic straining under load [13]. Coatings with high H^3/E^2 ratios may have higher fracture properties due to their high load-bearing capacity rather than their inherent strength [13]. It can be seen from Table 3 that the $Ti_{0.54}Cr_{0.46}N$ coating with the maximum hardness also has the highest H^3/E^2 value both among TiCrN coatings of other compositions and in comparison with TiN and CrN mononitride coatings. It is likely that the composition of the $Ti_{0.54}Cr_{0.46}N$ coating is optimum in terms of both the Ti/Cr element ratio and the content of crystalline phases.

The curves of variation of the friction coefficient (μ) with sliding distance are shown in Fig. 2. At the initial stage of dry friction tests ($\sim$ 0−25 m), coefficient μ of the

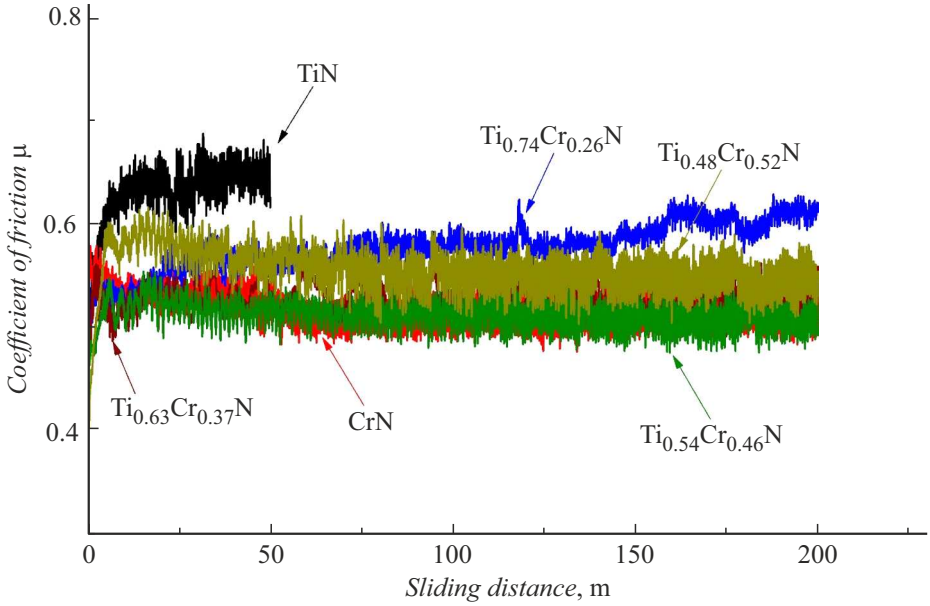

Figure 2. Curves of variation of the friction coefficient (μ) with sliding distance.

Table 3. Physical, mechanical, and tribological properties of the studied coatings (hardness H, elastic modulus E, hardness/elastic modulus ratio — H/E and H^3/E^2, and friction coefficient μ)

Sample	H, GPa	E, GPa	H/E	H^3/E^2, GPa	μ
TiN	30.8 ± 2.9	373.1 ± 34.5	0.08	0.21	0.631
CrN	23.8 ± 1.6	287.3 ± 9.8	0.08	0.16	0.519
$Ti_{0.74}Cr_{0.26}N$	31.6 ± 1.1	381.6 ± 6.6	0.08	0.22	0.577
$Ti_{0.63}Cr_{0.37}N$	32.6 ± 2.7	377.7 ± 42.8	0.09	0.24	0.530
$Ti_{0.54}Cr_{0.46}N$	37.4 ± 2.2	414.4 ± 25.1	0.09	0.30	0.512
$Ti_{0.48}Cr_{0.52}N$	32.2 ± 0.4	364.7 ± 7.7	0.09	0.25	0.556

studied TiCrN, TiN, and CrN coatings increased sharply to a stable state. The μ curve of the coating with the $Ti_{0.74}Cr_{0.26}N$ composition was the exception: after 150 m of testing, a sudden increase in μ was observed in this case. According to [14], the friction process may be divided into two stages: breaking-in and the steady-state regime. In addition, the initial period of breaking-in was characterized in [15], and it was reported that a rapid change in friction coefficient indicates the onset of coating wear. Figure 2 and Table 3 make it clear that the TiN mononitride coating had the maximum friction coefficient (0.631), while the minimum coefficient (0.512) corresponded to the $Ti_{0.54}Cr_{0.46}N$ coating, which had the best physical and mechanical characteristics. It is important to note that the determined friction coefficients of the studied coatings are significantly lower than the μ value for the original Cr12MoV steel (0.762).

Thus, the obtained data revealed that the variation of chromium content has a significant effect on the phase composition; crystal structure parameters; and physical, mechanical, and tribological properties of $Ti_{1-x}Cr_xN$ coatings. The $Ti_{0.54}Cr_{0.46}N$ coating composition is optimum in terms of both the ratio of Ti and Cr elements and the content of crystalline phases. Combined with a reduced CSR size and increased microstrain values, this makes its physical, mechanical, and tribological characteristics the best among the studied TiCrN coatings of other compositions and favorable compared to the parameters of mononitride TiN and CrN coatings.

Funding

This study was carried out under the state assignment of the Ministry of Science and Higher Education of the Russian Federation (project No. FWRM-2025-0001).

Conflict of interest

The authors declare that they have no conflict of interest.

References

[1] A.I. Men'shakov, D.R. Emlin, Tech. Phys. Lett., **47**, 511 (2021). DOI: 10.1134/S1063785021050254.
[2] T. Narayana, S.S. Saleem, Trib. Int., **193**, 109348 (2024). DOI: 10.1016/j.triboint.2024.109348
[3] A. Vorontsov, A. Filippov, N. Shamarin, E. Moskvichev, O. Novitskaya, E. Knyazhev, Yu. Denisova, A. Leonov, V. Denisov, S. Tarasov, Metals, **12** (10), 1746 (2022). DOI: 10.3390/met12101746
[4] A. Filippov, A. Vorontsov, N. Shamarin, E. Moskvichev, O. Novitskaya, E. Knyazhev, Yu. Denisova, A. Leonov, V. Denisov, S. Tarasov, Metals, **12** (12), 2046 (2022). DOI: 10.3390/met12122046
[5] A.A. Leonov, Yu.A. Denisova, V.V. Denisov, M.S. Syrtanov, A.N. Shmakov, V.M. Savostikov, A.D. Teresov, Coatings, **13** (2), 351 (2023). DOI: 10.3390/coatings13020351
[6] G. Mendoza-Leal, C. Hernandez-Navarro, J. Restrepo, M. Flores-Martinez, E. Rodríguez, E. García, MRS Adv., **3**, 3675 (2018). DOI: 10.1557/adv.2018.605
[7] S. Mohapatra, M.-S. Oh, Appl. Sci., **15** (5), 2466 (2025). DOI: 10.3390/app15052466
[8] O.I. Posylkina, S.D. Latushkina, I.A. Sechko, A.A. Vozniakovskii, E.A. Bogacheva, Tech. Phys., **70** (2), 255 (2025). DOI: 10.61011/TP.2025.02.60822.296-24.
[9] V.M. Savostikov, Yu.A. Denisova, V.V. Denisov, A.A. Leonov, S.V. Ovchinnikov, M.V. Savchuk, Russ. Phys. J., **64**, 2219 (2022). DOI: 10.1007/s11182-022-02580-x.
[10] K.H. Lee, C.H. Park, Y.S. Yoon, J.J. Lee, Thin Solid Films, **385** (1-2), 167 (2001). DOI: 10.1016/S0040-6090(00)01911-8
[11] C.X. Tian, Ch. Zou, Z.S. Wang, B. Yang, D.J. Fu, V.O. Pelenovich, A. Tolstogouzov, Int. J. Nanosci. Nanotechnol., **16** (4), 259 (2020). https://www.ijnnonline.net/article_47980.html
[12] A.D. Pogrebnjak, V.M. Beresnev, O.V. Bondar, Ya.O. Kravchenko, B. Zhollybekov, A.I. Kupchishin, Tech, Phys. Lett., **44** (2), 98 (2018). DOI: 10.21883/PJTF.2018.03.45575.16826 [A.D. Pogrebnjak, V.M. Beresnev, O.V. Bondar, Ya.O. Kravchenko, B. Zhollybekov, A.I. Kupchishin, Tech. Phys. Lett., **44** (2), 98 (2018). DOI: 10.1134/S1063785018020098].
[13] B.D. Beake, Surf. Coat. Technol., **442**, 128272 (2022). DOI: 10.1016/j.surfcoat.2022.128272].
[14] H.M. Cao, X. Zhou, X.Y. Li, K. Lu, Trib. Int., **115**, 3 (2017). DOI: 10.1016/j.triboint.2017.05.027].
[15] C.D. Rivera-Tello, E. Broitman, F.J. Flores-Ruiz, J. Perez-Alvarez, M. Flores-Jiménez, O. Jiménez, M. Flores, Coatings, **10** (3), 263 (2020). DOI: 10.3390/coatings10030263

Translated by D.Safin